Thickness Difference: A New Filtering Tool for Quantitative Electron Diffraction

Philip N. H. Nakashima*

Department of Materials Engineering, Monash University, Clayton Vic 3800, Australia
Monash Centre for Electron Microscopy, Monash University, Clayton Vic 3800, Australia

(Received 23 May 2007; published 20 September 2007)

A new way of filtering electron diffraction patterns has been discovered. Patterns from slightly different specimen thicknesses beyond the mean free path for inelastic scattering are subtracted. Only thickness sensitive information (dominantly elastic) remains. Thermal diffuse scattering and Borrmann effects are removed in addition to the inelastic signal eliminated by conventional energy filtering. One application is quantitative convergent beam electron diffraction without an energy filter. Structure factors for $\alpha - Al_2O_3$ have been measured with an average uncertainty of 0.25%.

DOI: 10.1103/PhysRevLett.99.125506 PACS numbers: 61.14.Lj, 34.80.−i

Electrons scatter 3 to 4 orders of magnitude more strongly from matter than other forms of radiation. Quantitative convergent beam electron diffraction (QCBED) was developed to exploit this sensitivity in order to probe chemial bonding and atomic structure in crystals [1–21]. The technique uses elastic scattering theory for fast electrons to simulate CBED patterns that can be matched to experimental ones. The fit is optimized by refining the parameters to which a pattern is most sensitive including the Fourier coefficients of the crystal potential (structure factors) corresponding to reflections at or near the Bragg condition.

QCBED pattern-matching refinements are ill constrained if the specimen thickness, H, is not equivalent to several extinction lengths, $\xi_{\mathbf{g}}$, of the reflections being matched, $\mathbf{g}$. This condition must be met to ensure enough turning points in a CBED pattern's intensity distribution. Because the mean free path for inelastic scattering, λ, is of the same order as extinction lengths of low order reflections, a suitable pattern for QCBED will have a significant inelastic signal. The earliest practitioners painstakingly minimized or subtracted the inelastic component prior to pattern matching with elastic scattering theory [2,3]; however, the enormous effort required slowed development of the field.

The invention of energy filtered transmission electron microscopy revived QCBED [4–21]. Data can now be captured within ± 2 eV about zero energy loss; however, this does not exclude thermal diffuse scattering (TDS) from phonons (tens of meV). Such tiny energy losses are well within the energy spread of the incident beam in even the latest monochromated TEMs and therefore, irrespective of hardware, a background remains.

Many have treated TDS in QCBED as a constant background for each reflection [6,8,10,11,13,16,19], while others have tried to account for its structure [3,14,17,20]. Recent work has shown the possibility of calculating the intensity distribution due to TDS and subtracting it from the experimental CBED data prior to pattern matching [22]. Incorporating inelastic scattering calculations into iterative pattern matching, however, remains computationally prohibitive.

This work opens QCBED to all TEMs, irrespective of energy filtering hardware, by demonstrating a simple new technique for filtering electron diffraction patterns using the specimen thickness alone. It takes advantage of the cross section for inelastic scattering of electrons, $K \propto 1 - e^{-H/\lambda}$ [23] where $H > \lambda$ because $H > \xi_{\mathbf{g}}$ for QCBED and $\xi_{\mathbf{g}} \approx \lambda$ for low order $\mathbf{g}$, as previously discussed. Thus, a small change in thickness, ΔH, results in only a small change in K. In contrast, the elastic signal is far more sensitive to a small ΔH. The present technique subtracts two CBED patterns taken from slightly different specimen thicknesses, thereby canceling the thickness insensitive components of the signal, i.e., most inelastic scattering and Borrmann-like effects [24]. The difference pattern is made up almost entirely of the elastic rocking curves from each component CBED pattern, allowing QCBED pattern-matching refinements based on elastic scattering theory. Trials on α-Al_2O_3 yield structure factor measurements with an average uncertainty of 0.25% and $<0.1\%$ in some cases, across a range of experimental conditions. The results agree with conventional energy filtered QCBED and are on average more precise.

The thickness difference CBED technique is summarized in Fig. 1. The inelastic background yields the keys to its own elimination, namely, higher order Laue zone (HOLZ) and Kikuchi lines. Selected segments (boxed in Fig. 1) are matched between the patterns while refining geometric distortion corrections that transform the thinner pattern into alignment with the thicker one. Prior to subtraction, the thinner pattern is scaled to equalize the background counts in the two patterns (measured from the boxed background segments). This scaling is typically very small (about 3% for $\Delta H/\bar{H} \approx 0.1$, $\bar{H}/\lambda \approx 2$, and $\lambda \approx 1000$ Å [25–27], considering $K \propto 1 - e^{-H/\lambda}$). Profiles in the as-captured data of Fig. 1 show the significance of the inelastic signal. The corresponding profiles in the difference pattern show that this background is almost completely eliminated.

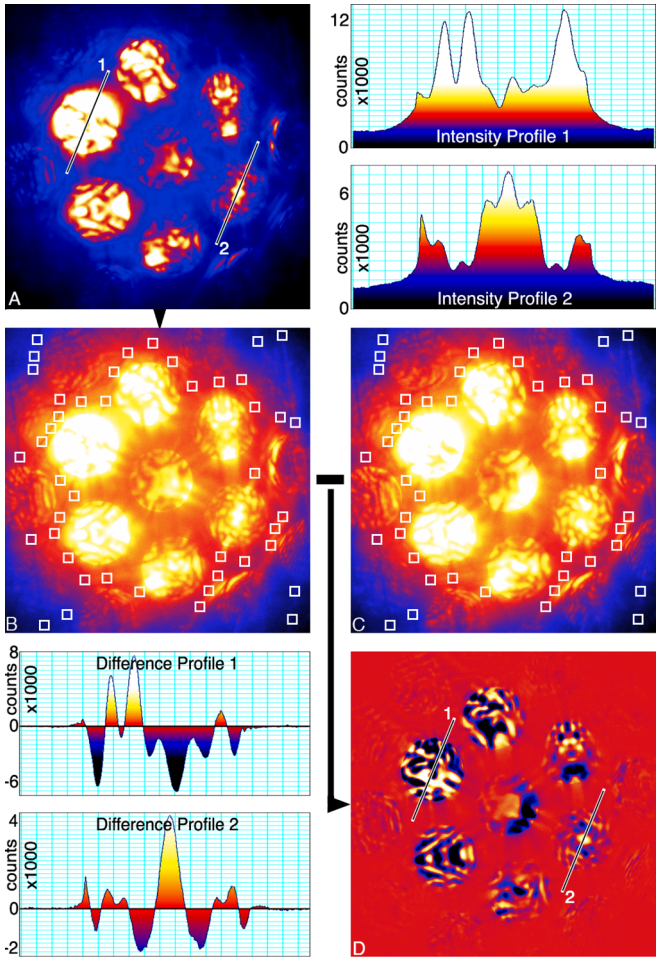

FIG. 1 (color online). The process of obtaining a thickness difference CBED pattern. (A) An unfiltered CBED pattern from near the [− 441] zone of α-Al_2O_3. Kikuchi and HOLZ line features are boxed (B) for alignment with the same features in a second pattern (C) from a thinner part of the specimen. Pattern C is aligned with B by matching the positions of the boxed features. The contrast in B and C is set $\propto$ ln(intensity) to make features in the background more visible in this figure. Pattern C is normalized with respect to B by comparing background intensities integrated over the boxed regions, prior to generating the difference pattern (D). Two intensity profiles from the thicker unfiltered CBED pattern show significant diffuse backgrounds outside the reflections. The corresponding profiles from the thickness difference pattern show that almost no background remains after subtraction.

Close scrutiny reveals that the remnant background outside the discs has a structure continuing from the intensity differences within the discs. This indicates plasmon scattering, which has essentially the same intensity distribution as the elastic scattering [3,28]. The effect is a slight amplification (without affecting the distribution) of the difference signal that would be obtained with only elastic scattering. QCBED pattern matching is unhindered as the added signal is incorporated in normalizing the calculated patterns to the experimental data.

CBED patterns aligned in reciprocal space, as in Fig. 1, will have relative shifts in disc position if the crystal orientation changes between regions of differing specimen thickness. The resulting imperfect overlap of discs in generating the difference pattern is treated by masking out the nonoverlapped segments when preparing the data for pattern matching. The nonoverlapping segments generally account for less than 5% of the total disc area.

CBED patterns from three different specimen thicknesses, $H_1 > H_2 > H_3$, allow a permuted triplet of difference data to be generated, i.e., $\{(H_1 - H_2), (H_1 - H_3), (H_2 - H_3)\}$. The procedure of Fig. 1 need be carried out only twice, i.e., for patterns 1 and 2 as well as 1 and 3, because the separately aligned patterns (2 and 3) share a common datum (pattern 1). This makes the thickness parameters interdependent as each one affects two of the difference patterns in the triplet, acting in conjunction with each of the other thickness parameters. This reduces correlations between structure factor and thickness parameters that are ever present in conventional QCBED where each pattern being matched has an independent thickness parameter. All experimental data used for pattern matching were prepared as difference triplets.

Pattern matching was performed using Zuo's Bloch-wave program, REFINECB [4,6], modified to calculate and match the permuted differences of three CBED patterns with the experimental input. In this regime, there is a threefold increase in the amount of data being matched, at the cost of only two additional refinement parameters (H_2 and H_3). The increase in computing time is very small as thickness only comes into the calculation of diffracted intensities after the scattering matrix diagonalization—by far the most expensive process. The thickness difference method is also suited to multislice algorithms as a thickness series is intrinsic to this formalism.

An example of pattern-matching input and output for thickness difference QCBED is given in Fig. 2. The difference data produced in Fig. 1 forms the first column of the experimental triplet. It is difficult to see discrepancies between the experimental and refined theoretical thickness difference patterns without the error map. The present results were obtained after 2 cycles of the distortion correction technique of [21], which is easily adapted from conventional QCBED to the difference technique.

For this work, [001] and [100] wedges of α-Al_2O_3 with impurity levels <20 ppm were tripod polished to 1.5° convergence. Additionally, specimens were produced by crushing, resulting in flakes with surface normals near [301] and [−441]. Unfiltered CBED patterns were collected at 120, 160, and 200 kV using a Philips CM20 and image plates as well as a JEOL 2011 with a Gatan Ultrascan 1000 CCD camera. Thickness series CBED data were collected for a number of different incident beam directions near each zone axis, thereby varying the combinations of different structure factors strongly influencing each series of patterns. The instrumental point

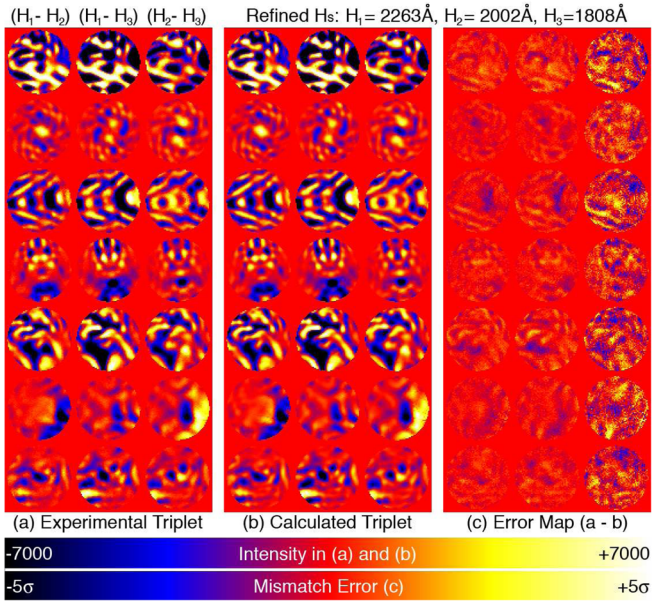

FIG. 2 (color online). An example triplet of thickness difference CBED patterns (unfiltered), matched with elastic scattering theory using a modified version of Zuo's Bloch-wave program, REFINECB [4,6]. The experimental data (a) is difficult to distinguish from the optimized theoretical intensity differences (b) without the error map (c) expressed in units of standard uncertainty in the experimental data.

spread function was measured and deconvoluted from the as-captured patterns according to the method of [29].

The results of some of the pattern-matching refinements carried out so far on thickness difference CBED data from α-Al_2O_3 are given in Table I. The means of the structure factors measured by this method generally agree with those from conventional energy filtered QCBED to within 1 or 2 standard uncertainties. The latter values are the culmination of previously published QCBED studies of α-Al_2O_3 [16,19,21].

Comparing the experimental measurements with structure factors calculated using the independent atom model (IAM, in which there is no chemical bonding), shows that the thickness difference and conventional QCBED approaches generally measure the same degrees of change in structure factor due to chemical bonding effects. However, for the higher order structure factors such as V_{220} and V_{214}, this is disputable. If one argues that the discrepancies between the means of both experimental techniques could largely be due to the presence of TDS in conventional QCBED and its absence in the thickness difference technique, then this would suggest that the true value of these structure factors is in fact much closer to the IAM value than suggested by conventional QCBED. Applying the thickness difference approach to energy filtered CBED data is required to clarify this conjecture and remains for a more technical paper [30].

In this work, each structure factor was measured between 6 and 72 times allowing a mean value and deviations of individual measurements to be determined. Expressed as percentages of their corresponding means, all of the structure factor measurement deviations were used to compile a histogram showing the general uncertainty of the technique. Figure 3 shows two such histograms, the first composed of 396 measurements of 21 independent structure factors using conventional energy filtered QCBED and the second summarizing 414 measurements of 13 independent

TABLE I. Structure factor, thickness and electron energy measurements using the thickness difference technique and unfiltered CBED patterns. Individual measurement uncertainties (given in the last 1 or 2 significant figures in brackets) were estimated from multiple refinements of each data set using different subsets of pixels making up each difference pattern. Mean values represent all 22 thickness difference refinement sets, of which only 8 are shown in the present table. Uncertainties in the mean values represent the spread of structure factor measurements across all 22 data sets refined (not just the 8 shown here). The same approach was adopted for the conventional energy filtered QCBED structure factor measurements given for comparison at the bottom of the table. These values resulted from the most recent refinements of data from previously published work [16,19,21].

Zone	e^- energy	Crystal thickness (Å)			Structure factors (volts)						
$[uvw]$	(keV)	H_1	H_2	H_3	{104}	{110}	{113}	{018}	{214}	{030}	{220}
[001]	200.80(7)	2535(5)	2298(2)	2136(1)		2.910(3)				4.868(9)	0.867(4)
[001]	200.85(19)	3026(3)	2963(2)	2836(1)		2.904(1)				4.862(5)	0.868(4)
[100]	119.99(27)	2247(4)	2147(3)	2023(3)	−4.033(5)					4.883(9)	
[301]	162.13(5)	1211(1)	1122(1)	1024(1)			−3.226(3)			4.876(6)	
[301]	162.04(9)	1239(1)	1147(9)	1074(1)			−3.221(4)				
[−441][a]	162.41(6)	2264(2)	2003(2)	1809(1)	−4.036(4)	2.890(6)		1.392(4)	−2.246(5)		
[−441]	162.31(18)	1450(1)	1383(1)	1287(1)	−4.036(3)				−2.211(5)		0.871(5)
[−441]	162.31(11)	1237(1)	1992(1)	1114(1)				1.385(6)			0.869(8)
	Mean				−4.036(5)	2.900(10)	−3.225(10)	1.386(6)	−2.238(11)	4.874(9)	0.871(9)
	Energy filtered QCBED				−4.022(8)	2.924(19)	−3.217(13)	1.394(7)	−2.209(1)	4.865(6)	0.896(6)
	Independent atom model				−3.921	2.591	−3.546	1.425	−2.225	4.840	0.867

[a]Results from experimental data shown in Figs. 1 and 2.

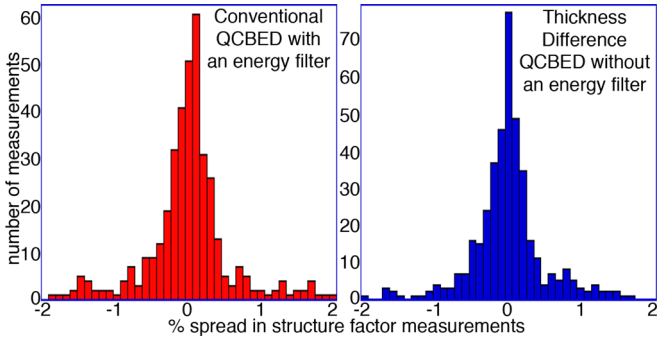

FIG. 3 (color online). Histograms showing the general uncertainty associated with conventional energy filtered QCBED and the thickness difference approach using unfiltered CBED patterns. Each histogram was generated from the percentage deviation of each individual structure factor measurement from the mean of all measurements of that particular structure factor and summing over all structure factors measured.

structure factors using the thickness difference approach and unfiltered CBED patterns. The sets of structure factors measured by each method spanned the same angular range with $\frac{\sin\theta}{\lambda} \leq 0.5$ Å^{-1}.

The noticeable reduction in spread using the thickness difference approach accompanies a mean deviation or uncertainty of 0.25% compared to 0.34% for conventional QCBED. Both of these results are less than the disagreement between different theoretical calculations (density functional theory and periodic Hartree-Fock) of the same structure factors, shown in [21].

Removing TDS via the thickness difference technique accounts for some of the improvement in precision over conventional QCBED. The reduced correlation between thickness and structure factor parameters due to the permutative coupling in difference triplets plus the increased number of data points is the other dominant factor in this improvement. An analysis of the pattern-matching process with difference patterns both parametrically and in terms of the iterative path to the best fit is in progress and will be discussed in a more technical paper covering all aspects of the present technique [30].

In conclusion, all results presented here were gained from CBED patterns obtained without an energy filter. This work demonstrates that thickness difference QCBED opens the field of accurate electronic structure measurement to all TEM facilities in a practical manner. Furthermore, it improves upon the precision of conventional energy filtered QCBED as shown in the reduced average uncertainty of the measured structure factors. Applying the thickness difference approach to energy filtered data is expected to enhance QCBED even further.

The author thanks Professor J. M. Zuo, Associate Professor J. Etheridge, Professor A. F. Moodie, Dr. V. A. Streltsov, Associate Professor A. W. S. Johnson, the Australian Research Council (No. DP0346828), the Victorian Partnership for Advanced Computing, and the Australian Partnership for Advanced Computing.

*Philip.Nakashima@eng.monash.edu.au

[1] C. H. MacGillavry, Nature (London) **145**, 189 (1940).
[2] P. Goodman and G. Lehmpfuhl, Acta Crystallogr. **22**, 14 (1967).
[3] R. Voss, G. Lehmpfuhl, and P. J. Smith, Z. Naturforsch. **35A**, 973 (1980).
[4] J. M. Zuo, J. C. H. Spence, and M. O'Keeffe, Phys. Rev. Lett. **61**, 353 (1988).
[5] D. M. Bird and M. Saunders, Ultramicroscopy **45**, 241 (1992).
[6] J. M. Zuo, Acta Crystallogr. Sect. A **49**, 429 (1993).
[7] C. Deininger, G. Necker, and J. Mayer, Ultramicroscopy **54**, 15 (1994).
[8] R. Holmestad, J. M. Zuo, J. C. H. Spence, R. Høier, and Z. Horita, Philos. Mag. A **72**, 579 (1995).
[9] L. M. Peng and J. M. Zuo, Ultramicroscopy **57**, 1 (1995).
[10] M. Saunders, D. M. Bird, N. J. Zaluzec, W. G. Burgess, A. R. Preston, and C. J. Humphreys, Ultramicroscopy **60**, 311 (1995).
[11] M. Saunders, D. M. Bird, O. F. Holbrook, P. A. Midgley, and R. Vincent, Ultramicroscopy **65**, 45 (1996).
[12] J. M. Zuo, M. O'Keeffe, P. Rez, and J. C. H. Spence, Phys. Rev. Lett. **78**, 4777 (1997).
[13] M. Saunders, A. G. Fox, and P. A. Midgley, Acta Crystallogr. Sect. A **55**, 471 (1999).
[14] K. Tsuda and M. Tanaka, Acta Crystallogr. Sect. A **55**, 939 (1999).
[15] J. M. Zuo, M. Kim, M. O'Keeffe, and J. C. H. Spence, Nature (London) **401**, 49 (1999).
[16] V. A. Streltsov, P. N. H. Nakashima, and A. W. S. Johnson, J. Phys. Chem. Solids **62**, 2109 (2001).
[17] K. Tsuda, Y. Ogata, K. Takagi, T. Hashimoto, and M. Tanaka, Acta Crystallogr. Sect. A **58**, 514 (2002).
[18] B. Jiang, J. M. Zuo, N. Jiang, M. O'Keeffe, and J. C. H. Spence, Acta Crystallogr. Sect. A **59**, 341 (2003).
[19] V. A. Streltsov, P. N. H. Nakashima, and A. W. S. Johnson, Microsc. Microanal. **9**, 419 (2003).
[20] Y. Ogata, K. Tsuda, Y. Akishige, and M. Tanaka, Acta Crystallogr. Sect. A **60**, 525 (2004).
[21] P. N. H. Nakashima, J. Appl. Crystallogr. **38**, 374 (2005).
[22] K. Omoto, K. Tsuda, and M. Tanaka, J. Electron Microsc. **51**, 67 (2002).
[23] R. F. Egerton, *Electron Energy Loss Spectroscopy in the Electron Microscope* (Plenum Press, New York and London, 1996), 2nd ed.
[24] P. Goodman, Z. Naturforsch. **28A**, 580 (1973).
[25] T. Malis, S. Cheng, and R. F. Egerton, J. Electron Microsc. Tech. **8**, 193 (1988).
[26] D. R. Mitchell and B. Schaffer, Ultramicroscopy **103**, 319 (2005).
[27] D. R. Mitchell, J. Microsc. **224**, 187 (2006); http://www.felmi-zfe.tugraz.at/dm_scripts/dm_scripts/freeware/programs/Mean-Free-Path-Estimator.htm.
[28] S. L. Dudarev, L.-M. Peng, and M. J. Whelan, Phys. Rev. B **48**, 13 408 (1993).
[29] P. N. H. Nakashima and A. W. S. Johnson, Ultramicroscopy **94**, 135 (2003).
[30] P. N. H. Nakashima (to be published).